

# Ganglion Cell Distribution and Retinal Resolution in the Florida Manatee, *Trichechus manatus latirostris*

ALLA M. MASS,<sup>1\*</sup> DARLENE R. KETTEN,<sup>2</sup> DANIEL K. ODELL,<sup>3</sup>  
AND ALEXANDER YA. SUPIN<sup>1</sup>

<sup>1</sup>Institute of Ecology and Evolution, Russian Academy of Sciences, Moscow, Russia

<sup>2</sup>Department of Otology and Laryngology, Harvard Medical School, Boston, Massachusetts

<sup>3</sup>Sea World Inc., 7007 Sea World Drive, Orlando, Florida

## ABSTRACT

The topographic organization of retinal ganglion cells was examined in the Florida manatee (*Trichechus manatus latirostris*) to assess ganglion cell size and distribution and to estimate retinal resolution. The ganglion cell layer of the manatee's retina was comprised primarily of large neurons with broad intercellular spaces. Cell sizes varied from 10 to 60  $\mu\text{m}$  in diameter (mean 24.3  $\mu\text{m}$ ). The retinal wholemounts from adult animals measured 446–501  $\text{mm}^2$  in area with total ganglion cell counts of 62,000–81,800 (mean 70,200). The cell density changed across the retina, with the maximum in the area below the optic disc and decreasing toward the retinal edges and in the immediate vicinity of the optic disc. The maximum cell density ranged from 235 to 337 cells per millimeter square in the adult retinae. Two wholemounts obtained from juvenile animals were 271 and 282  $\text{mm}^2$  in area with total cell numbers of 70,900 and 68,700, respectively (mean 69,800), that is, nearly equivalent to those of adults, but juvenile retinae consequently had maximum cell densities that were higher than those of adults: 478 and 491 cells per millimeter square. Calculations indicate a retinal resolution of  $\sim 19'$  (1.6 cycles per degree) in both adult and juvenile retinae. *Anat Rec*, 295:177–186, 2012. © 2011 Wiley Periodicals, Inc.

**Key words:** manatee; *Trichechus manatus*; eye; retina; ganglion cells; cell topography; cell size; retinal resolution; visual acuity

The Sirenia order includes the manatee, dugong, and the extinct Steller cow. Sirenians are adapted to salt and fresh water habitats and, unlike other marine mammals, are exclusively herbivorous. Consequently, they have a range of unique anatomical, physiological, and behavioral adaptations. Further, all species of the order are endangered. The West Indian manatee is a slow grazer that inhabits the coastal areas and rivers of the Caribbean basin (Bertram and Bertram, 1962; Hartman, 1979; Nowak, 1991). The Florida manatee, *Trichechus manatus latirostris*, is a subspecies of the West Indian manatee, *T. manatus*. Knowing more about their sensory abilities, including their visual abilities, is of interest not only for basic evolutionary research but also for planning strategies for conserving this highly endangered species.

The knowledge of the visual capabilities of the manatee is limited and contradictory (Bauer et al., 2003). In early investigations summarized by Walls (1942), the

Grant sponsor: Russian Foundation for Basic Research; Grant number: 10-04-00476.

\*Correspondence to: Alla M. Mass, 33 Leninsky Prospect, 119071 Moscow, Russia. E-mail: alla-mass@mail.ru  
Daniel K. Odell is currently affiliated with 3221 Blue Mesa Drive, Divide, CO 80814.

Received 28 January 2011; Accepted 17 June 2011

DOI 10.1002/ar.21470

Published online 1 October 2011 in Wiley Online Library (wileyonlinelibrary.com).

vision of the sirenians was estimated as “wretched” because of the myopic refraction in air, the lack of lenticular accommodation, and the reported paucity of retinal ganglion cells. According to Walls (1942), the manatee’s eye is adapted for underwater vision and more for sensitivity than discrimination. A more optimistic suggestion based on the visual behavior was that the manatee relies considerably on the visual exploration of the environment (Hartman, 1979).

The first experimental investigation of the manatee’s vision was carried out by Piggins et al. (1983) in the Amazonian manatee *T. inunguis*. Their data showed that the emmetropic eye of *T. inunguis* is capable of focusing and tracking objects at a distance of a meter or more under water, but no evidence was found for tracking objects above water. The authors suggested that the eye of *T. inunguis* is adapted primarily for underwater vision. Griebel and Schmidt found that West Indian manatees *Trichechus manatus latirostris* were capable of both color discrimination (Griebel and Schmidt, 1996) and brightness discrimination with a moderate differential threshold of about 0.3 (Griebel and Schmidt, 1997).

The manatee’s visual system possesses some unusual anatomical features. Contrary to the majority of mammals that have avascular corneae, blood vessels have been reported throughout the manatee cornea (Harper et al., 2005). Another unusual feature of the manatee’s visual system is that the ciliary body contains no muscle fibers (West et al., 1991; Samuelson et al., 1994; Natiello et al., 2005). Further, the angioarchitecture of the ciliary body of the manatee is unique compared to those examined in terrestrial mammals. Previous authors surmised that these structures allow for accommodation by controlling the pressure exerted on the vessels associated with aqueous humor dynamics. This regulation may therefore assist accommodation in lieu of the absent ciliary body musculature.

The manatee’s eye is reported to lack a definite tapetum (West et al., 1991). However, manatees have eyes equipped with a rod-dominant retina (Cohen et al., 1982), which may provide good sensitivity despite the lack of a tapetum (Griebel and Schmidt, 1997).

With respect to visual resolution, prior to this study, there was only one behavioral investigation studying underwater visual acuity in the Florida manatee *Trichechus manatus latirostris* (Bauer et al., 2003). This study reported substantial differences in the results for its two subjects with minimum angles of resolution of 56' and 21'.

Data on retinal organization in manatees are rare. The first description of the manatee’s retina was published by Pütter (1903). Rochon-Duvigneaud (1943) and Walls (1942) described the retina of the manatee and dugong as being solely equipped with rods. Later, Piggins et al. (1983) similarly indicated that the manatee’s *T. inunguis* retina has a structure typical of nocturnal animals and that cones are rare or absent. Ganglion cells were noted to be few in number, although no quantification of cell number was given.

A detailed description of the retina of *T. manatus* was made by Cohen et al. (1982), who reported fully developed layering of the retina. Using light and electron microscopy, they found both dominating rod-like photoreceptors and cone-like photoreceptors, and two types of cone cells, which is consistent with the color vision

results in later behavioral experiments by Griebel and Schmidt (1996). The results suggest the presence of dichromatic color vision based on two photoreceptor types, one with maximum sensitivity in the blue region of the spectrum and the other in the green region. Recent molecular investigation in the West Indian manatee *Trichechus manatus latirostris*, in which LWS and SWS cone opsin were cloned and sequenced and which revealed wavelengths of maximum absorbance of 555 and 410 nm, supports this conclusion (Newman and Robinson, 2006). It is noteworthy that dichromatic color vision is common to most diurnal mammals including elephants (Proboscidea) and hyraxes (Hirocoidea), the manatee’s closest terrestrial relatives (Ahnelt and Kolb, 2000). Expression of both the LWS and SWS cone opsin in the manatee retina is unique among marine mammals; cetaceans and pinnipeds only express a LWS cone opsin (Griebel and Peichl, 2003).

Until now, little has been known concerning the retinal ganglion cell morphology, topography, and distribution in manatees. Although preliminary data for some of these subjects have been previously published (Mass et al., 1997), this article presents comprehensive, detailed results for all available specimens. Retinal ganglion cell distribution in wholemounts provides quantitative estimates of the retinal resolution, which is a crucial factor in visual resolution. Cell distributions also demonstrate which parts of the visual field are most important for visual orientation of the animal. Using this method, retinal resolution has been estimated in many terrestrial (rev. Pettigrew et al., 1988) and marine mammals (Landau and Dawson, 1970; Murayama et al., 1992, 1995; Supin et al., 2001; Welsch et al., 2001; Mass and Supin, 2003, 2005, 2010; Hanke et al., 2009). To date, however, there is no investigation of this kind on manatee retinæ. Therefore, the purpose of this study was to investigate ganglion cell topography and cell density distribution in retinal wholemounts of the Florida manatee *Trichechus manatus latirostris*. The primary intent of the study was to obtain topographic data to localize areas of highest ganglion cell concentration and to assess retinal resolution. Ganglion cell sizes were studied in various parts of the retina as well.

## MATERIALS AND METHODS

Six eyes were collected from three adult Florida manatees, *T. manatus latirostris*, of 270–290 cm body length (SWF-TM-7918-B, female; SWF-TM-9526B, female; and SWF-TM-9529B, female) and from one juvenile animal, 130 cm body length (SWF-TM-9410B, male).

The eyes were removed postmortem and preserved in 10% buffered formalin. To estimate the positions of important optical points and the posterior nodal distance, one eye of an adult animal was frozen and sectioned longitudinally, with the axis passing through the center of the cornea and the optic nerve head. Measurements were made from photographs of these sections.

Four eyes from adults and two eyes from the juvenile animal were processed for retinal wholemounts. Wholemounts were prepared using Stone’s (1981) method with some modifications (Mass and Supin, 1995, 2003). Before the eyeball was excised, its orientation in the orbit was noted and marked by a small cut on the dorsal pole. After eye excision, the iris, lens, and vitreous body of the

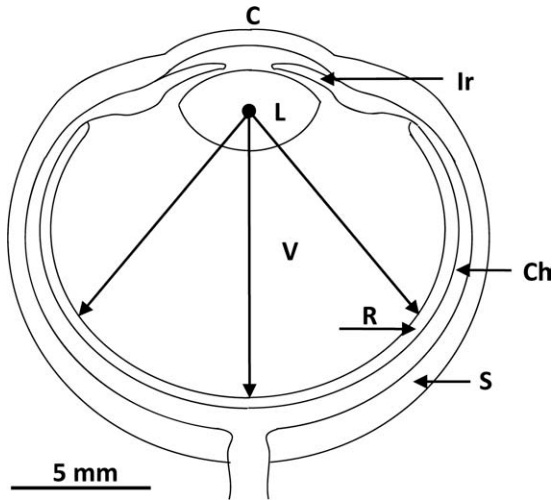


Fig. 1. Horizontal section of a manatee's eye (redrawn from a photograph). C, cornea; Ir, iris; L, lens; Ch, choroid; R, retina; S, sclera. Arrows indicate the measured distances from the lens center to the center and points of  $\pm 30$ -degree angle from the center of the retina.

eye were removed, and the dorsal pole of the retina was again marked by a small cut. The retina was separated from the pigment epithelium and excised from the eyecup. Several peripheral radial cuts were made in the retina to flatten it. Subsequently, the retina was flat-mounted on a slide with the ganglion cell layer uppermost, weighted in 10% buffered formalin solution for several hours, and air dried. At this stage, the whole-mount dimensions were measured.

The retina was stained using a Nissl technique with 0.1% Cresyl violet. It was then dehydrated in graduated ethanol solutions, cleared with xylene, and mounted. The wholemount measurements were repeated at this stage to compare with values prior to dehydrating and staining. No significant changes were found in any wholemount; only minor shrinkage in narrow zones along the edges was found. Counts from these regions were not used in the preparation of retinal maps.

Ganglion cells were counted at 1-mm steps across the whole retina. At each position, the number of cells was counted in a 0.067-mm<sup>2</sup> sample, and the counts were converted to cells per millimeter square. These data were used to map the ganglion cell density distribution in the retina and to calculate the total number of ganglion cells. Smoothing of the maps was carried out by averaging the number of cells in blocks of 3 × 3 samples. Cell size was evaluated by measuring two perpendicular diameters of each cell, that is, the longest and shortest ones (defined as the minimal and maximal distances between opposite edges of the cell profile), and calculating the mean value.

**RESULTS**

**Eye Dimensions**

Figure 1 demonstrates a longitudinal section of a frozen manatee eye. Basic dimensions of the adult eye were as follows. Axial length between the external surfaces of the cornea and sclera was 16 mm. Equatorial nasotem-

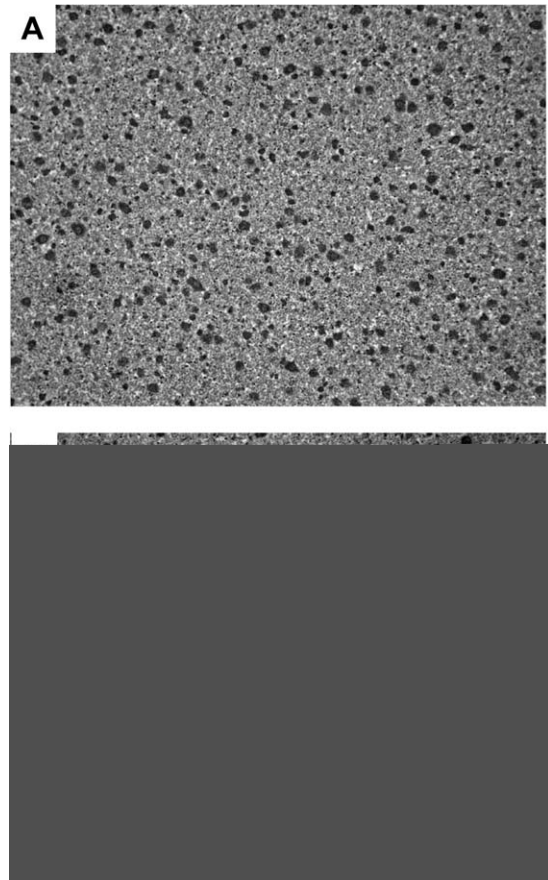


Fig. 2. Light micrograph from the ganglion cell layer of a Nissl-stained retinal wholemount of the manatee. (A) In an area of ganglion cell density with more than 200 cells per millimeter square. (B) In an area of ganglion cell density with less than 100 cells per millimeter square.

poral width was 17 mm. Internal eyecup diameter was 15 mm. The distance from the center of the lens to the center of the retina was 10.5 and 9 mm to points  $\pm 30$ -degree angle from the center. The cornea was round or slightly oval (vertical diameter longer) with a diameter of 6.5–7 mm. The iris was well developed. The pupil was slightly oval, the vertical axis longer. The lens was set forward, and the anterior chamber was shallow. Unlike the spherical lenses of cetaceans and pinnipeds, the lens in the manatee eye was more conventionally oblate or lenticular, about 3 mm along the axis and 5 mm in the transverse diameter. The sclera was of a constant width except in the region near the optic nerve where it was thickened.

The nonadult eyes were not sectioned because the material was limited. Both available eyes were used to prepare retinal wholemounts. However, external measurements before excising the retina as well as measurements of eyecups remaining after the excision provided the following dimensions: axial length between the external surfaces of the cornea and sclera was 12.5–13 mm, and the equatorial nasotemporal width was 13 mm. Internal eyecup diameter was 11–11.5 mm. The distance from the center of the lens to the retina was estimated to be ~8 mm.

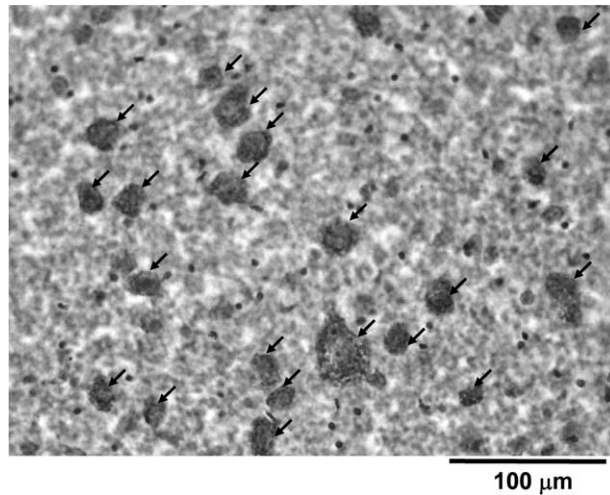


Fig. 3. Fragment of light micrograph from the ganglion cell layer of a Nissl-stained retinal wholemount of the manatee. Cells classified as ganglion cells are marked by arrows.

### Ganglion Cell Characteristics

Figures 2 and 3 illustrate ganglion cells in the ganglion cell layer of a Cresyl violet-stained wholemount. The ganglion cell layer of the manatee's retina consisted mainly of large neurons, separated by rather wide intercellular spaces.

Most cells were 14–30  $\mu\text{m}$  in size. No cell less than 10  $\mu\text{m}$  or larger than 60  $\mu\text{m}$  was found. The cells had abundant cytoplasm with well-stained Nissl granules (Fig. 3). The nucleus was lighter than the cytoplasm and had a clearly visible nucleolus. As a rule, the nucleus was large.

Most of the cells were polygonal; however, some cells had only one distinct process. Several cells were circular or ovoid with no identifiable process. Most of the cells were clearly identifiable as neurons and were assumed to be ganglion cells, but a small percentage of cells were difficult to categorize. Small cells (typically less than 10  $\mu\text{m}$  in size) with an irregular shape and a large lightly stained nucleus with visible nucleolus and narrow cytoplasmic rings were tentatively classified as amacrine cells. Small (about 5  $\mu\text{m}$ ), rounded, deeply stained cells were deemed neuroglia. Both the amacrine and neuroglial cells were excluded from further consideration.

### Ganglion Cell Size

A total of 2,000 cells were measured in three wholemounts obtained from adult animals. In each of the three wholemounts, ganglion cells sizes were measured in two samples located in different regions of the retina: in one of high cell density (more than 200 cells per millimeter square) and one with low cell density (less than 100 cells per millimeter square). Thus, six samples were measured in total.

Figure 4 shows the distributions of ganglion cells sizes in these six samples. Within the overall cell size range of 10–60  $\mu\text{m}$ , the majority of cells were of a size from 12 to 35  $\mu\text{m}$ .

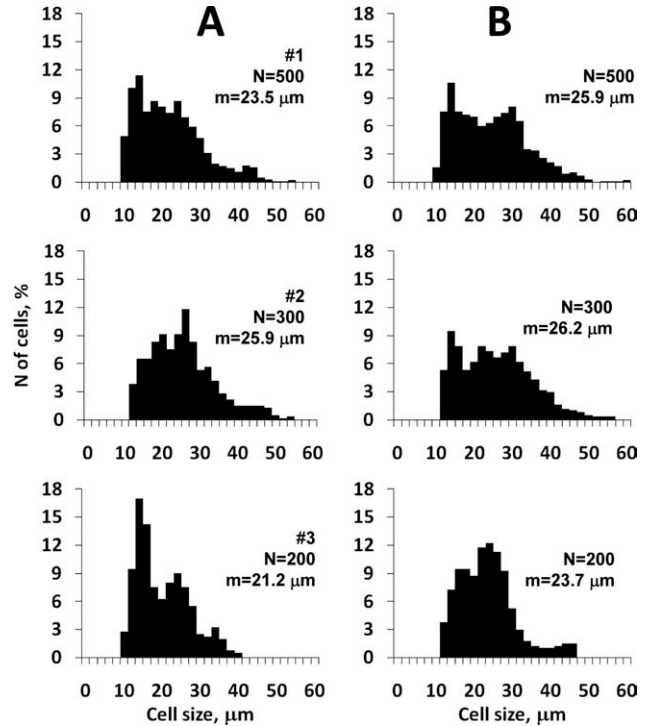


Fig. 4. Histograms of ganglion cell size distribution in six samples from three retinal wholemounts (# 1, 2, 3). (A) Samples from areas of ganglion cell density with more than 200 cells per millimeter square (below the optic disc). (B) Samples from areas of ganglion cell density with less than 100 cells per millimeter square (dorsal periphery).

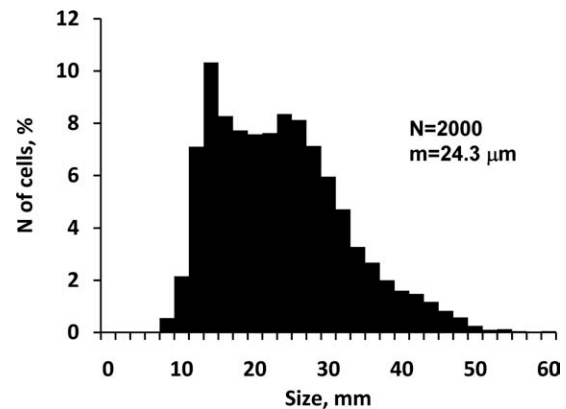


Fig. 5. Ganglion cell size distribution of the total cell population of six samples presented in Fig. 4.

The shape of the histograms was not singularly unimodal, although some were not truly bimodal either. Obviously bimodal distributions were #1B, #2B, and #3A, which had one peak at 12–14  $\mu\text{m}$  and another greater than 25  $\mu\text{m}$ , with a clear gap between them. In other cases, the gap consisted of a “plateau” or flattened region. This may indicate the presence of two common cell sizes, one 12–16 and one over 25  $\mu\text{m}$ .

The means varied slightly among the areas (from 21.2 to 26.2  $\mu\text{m}$ , Fig. 4). Although histograms of different

**TABLE 1. Retinal area, number of cells, and maximum cell density in the investigated wholemounts**

Wholemount number	Animal id.	Eye left/right	Retinal area (mm <sup>2</sup> )	Number of cells	Maximum cell density (cells per millimeter square)
1	SWF-TM 7918-B	L	484	72,500	292
2	SWF-TM 9526-B	L	494	81,800	337
3	SWF-TM 9526-B	R	501	64,500	281
4	SWF-TM 9529-B	L	446	62,000	235
	Mean #1:#4 (adults)		481	70,200	286
5	SWF-TM 9410-B	R	282	70,900	491
6	SWF-TM 9410-B	L	271	68,700	478
	Mean #5:#6 (juveniles)		277	69,800	485

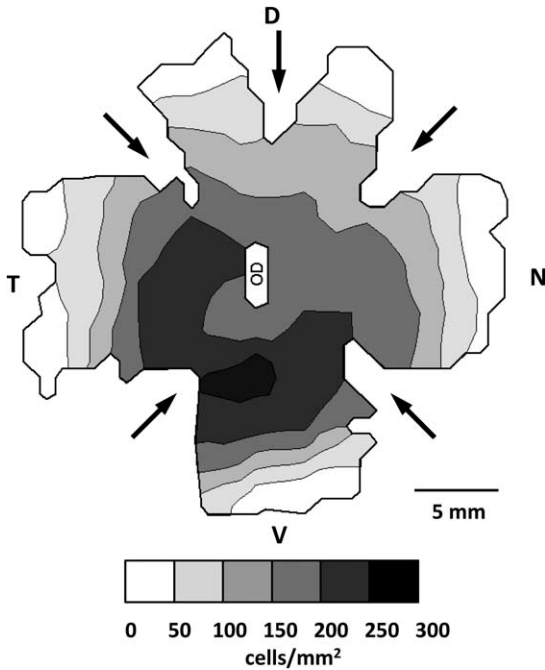


Fig. 6. Map of ganglion cell density in a retinal wholemount (adult animal, right eye, wholemount #3 according to Table 1). Cell density is designated according to the scale below. N, T, D, V, nasal, temporal, dorsal, and ventral poles of the retina; OD, optic disc.

samples were not isomorphic, we did not find any variation in their shape or means related to sample location. Therefore, all the adult histograms were pooled to obtain the overall cell size distribution and averages. The result is shown in Fig. 5. This averaged histogram also had two slightly pronounced peaks at 14 and 26  $\mu\text{m}$  with a mean of 24.3  $\mu\text{m}$ .

**Distribution and Number of Ganglion Cells**

**Adult animals.** The four retinal wholemounts obtained from adults ranged from 446 to 501 mm<sup>2</sup> in area (Table 1). The ganglion cell total in these wholemounts (rounded to 1,000) varied from 62,000 to 81,800 (mean 70,200) cells.

Ganglion cell distribution varied smoothly across the retina. A representative pattern of ganglion cell distribution derived from the ganglion cell counts throughout the retina is presented as a map in Fig. 6. This pattern

can be described as bell shaped; that is, cell density was higher at the central part of the retina and diminished toward the retinal borders. Near the optic disc, cell density diminished noticeably. The highest cell density was located below the optic disc, where it exceeded 250 cells per millimeter square in one case (in this particular wholemount, the maximum cell density was 280 cells per millimeter square). In different wholemounts, the peak cell density varied from 235 to 337 cells per millimeter square, mean 286 cells per millimeter square (Table 1).

The cell density distribution profile featured a smooth gradient in the cell density within a major part of the retina, and no sharply restricted area of high cell concentration could be identified. Only at the retinal periphery and near the optic disc did ganglion cell density fall markedly. For example, in the wholemount presented in Fig. 6, which had the highest cell density of 280 cells per millimeter square, the area in which cell density exceeded 150 cells per millimeter square occupied about a half of the retinal area.

This peculiarity of the cell density distribution is clearly visible when presented as plots of the distribution of trans-retinal lines crossing nasotemporally (Figs. 7A, 8A) and dorsoventrally (Figs. 7B, 8B). The plots demonstrate bell-shaped distributions in both the dorsoventral and nasotemporal directions. The smooth form of the plots is disrupted only near the optic disc where the density decreases.

This form of representation allows combined data from all four wholemounts to be shown as individual plots (Fig. 7) and interwholemount means with standard deviation (Fig. 8).

**Juvenile animals.** The two juvenile retinal wholemounts measured 282 and 271 mm<sup>2</sup> in area, mean 277 mm<sup>2</sup>, that is, 1.7 times less than the adult ones. The ganglion cell totals in the wholemounts were 70,900 and 68,700, mean 69,800, that is, very close to the values in the adult wholemounts.

Ganglion cell spatial distribution in the juvenile eyes was qualitatively similar to that in adult eyes. Both the retinal maps (one map is shown in Fig. 9) and the plots of cell distribution along the nasotemporal and dorsoventral lines (Fig. 10) show the same bell-shaped distribution with the maximum below the optic disc. Because the retinal area in juveniles was less than in adults and the overall number of cells was nearly the same, the cell densities were consequently higher in juveniles than in adults, with juvenile maximum densities of 491 and 478

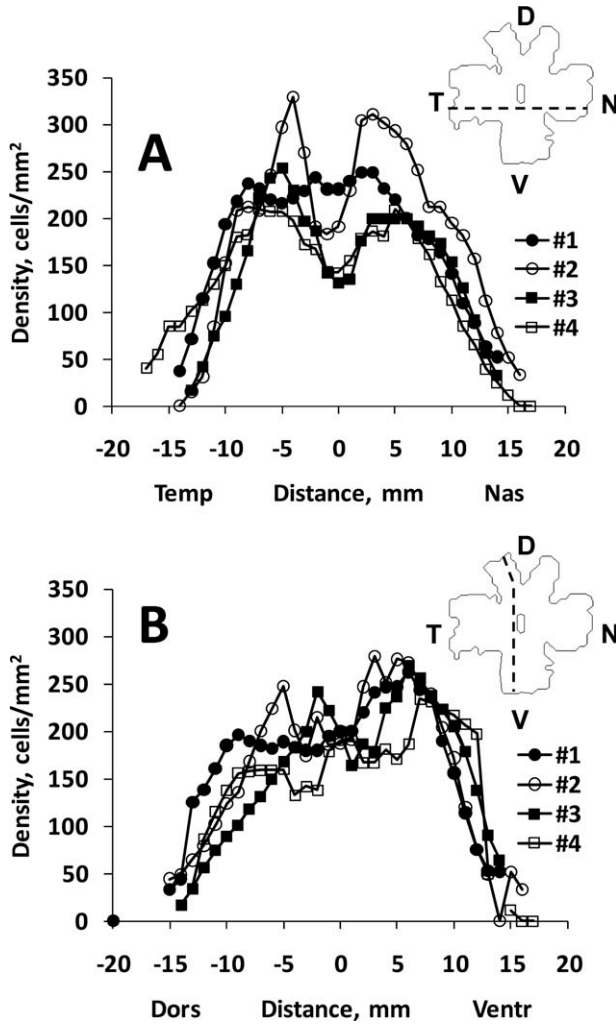


Fig. 7. Ganglion cell density distributions along a nasotemporal line below the optic disc (A) and along a dorsoventral line temporal of the optic disc (B). Plots obtained from four wholemounts (adults) are designated by different symbols. Inserted map contours exemplify the measurement transects in one of the wholemounts (#3 according to Table 1).

cells per millimeter square and an average of 485 cells per millimeter square.

**DISCUSSION**

**Identification of Ganglion Cells**

A study like the present one requires careful criteria to distinguish ganglion cells from amacrine and neuroglial cells. This study is the first investigation of wholemounts of the manatee retina. Therefore, no specific criteria for this species were available from earlier reports. We used well-developed criteria from multiple studies of other animals (Hughes, 1975; Stone, 1981; Wong et al., 1986; Wong and Hughes, 1987). Large soma size (more than 10  $\mu$ m), cytoplasm with irregularly stained Nissl granules, and nucleus with nucleolus were adopted as the critical features of ganglion cells. The observed consistently large size of ganglion cells in the

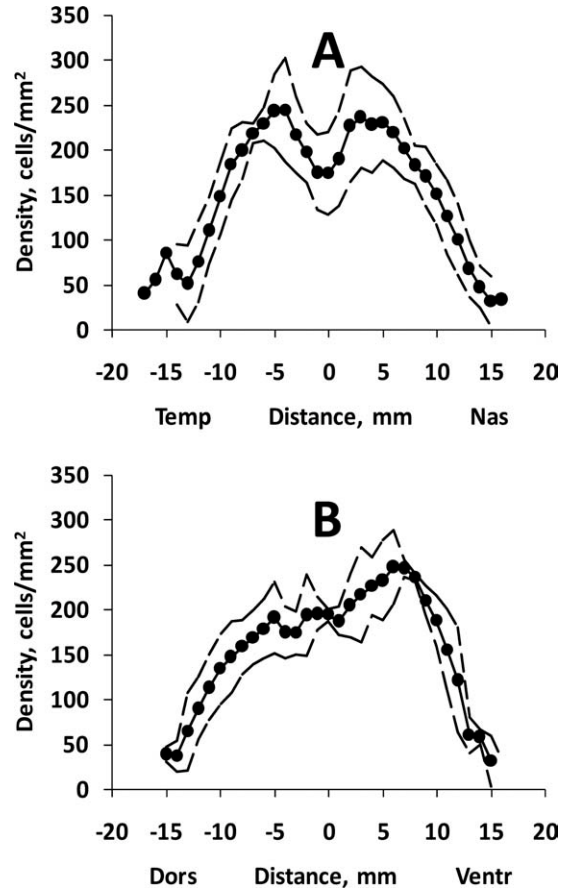


Fig. 8. Ganglion cell density distributions along nasotemporal lines below the optic disc (A) and along dorsoventral lines temporal of the optic disc (B). Averaged data (mean  $\pm$  SD) of four wholemounts presented in Fig. 7.

manatee helped to distinguish them from amacrine cells and neuroglia.

Cresyl violet staining (Nissl method) used in this study provides less exact identification of ganglion cells than some more modern methods, for example, retrograde tracing, but it is both applicable and reliable in postmortem extracted tissues, and this method is widely used for retinal wholemounts. Collin and Pettigrew (1988) have shown that the data of ganglion cell counts using Nissl method are consistent with the results from tracing methods. This method has also been used previously to count ganglion cells in other aquatic mammals, and the data obtained provided reliable estimates of the amount of the cells. For example, the total amounts of ganglion cells found in the retina of the Amazonian river dolphin *Inia geoffrensis* (Mass and Supin, 1989), bottle-nose dolphin *Tursiops truncatus* (Mass and Supin, 1995), and walrus *Odobenus rosmarus* (Mass, 1992) were close to the numbers of fibers in the optic nerve (Pütter, 1903; Morgane and Jacobs, 1972; Dawson, 1980; Dawson et al., 1982; Gao and Zhou, 1992). This suggests that the cell counts in our studies were adequate for reliable estimates. Although it is possible that some amacrine cells were referred to ganglion cells, it is unlikely to have influenced the total counts substantially. Thus, we

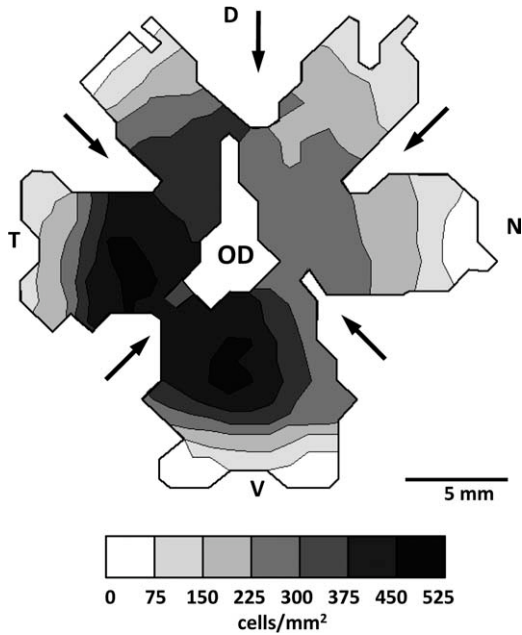


Fig. 9. Map of ganglion cell density in a retinal wholemount (juvenile animal, right eye, wholemount #5 according to Table 1). Conventions as in Fig. 6.

conclude that the method used is appropriate to study both the total number of cells and the cell density patterns in the manatee retina.

**Ganglion Cell Size**

The manatee’s retina contained mainly large ganglion cells with a mean cell size as large as 24.3  $\mu\text{m}$  and maxima as great as 60  $\mu\text{m}$ . Previously, Cohen et al. (1982) described even larger (up to 65–90  $\mu\text{m}$ ) cells in a related species, the West Indian manatee. We observed large cells in various regions of the retina irrespective of the cell density in these regions. With respect to large cell size, the manatee’s retina was similar to those of other aquatic mammals that also contained large ganglion cells (Dawson et al., 1982; Waller, 1982; Dral, 1983; Mass and Supin, 1986, 1995, 1999, 2003, 2005; Gao and Zhou, 1992; Murayama et al., 1992, 1995). Thus, it appears that large ganglion cells are a common feature of aquatic mammals contrary to reports for many terrestrial mammals, which typically have ganglion cells no larger than 25–30  $\mu\text{m}$  (Fukuda, 1977; Hughes, 1981; Oyster et al., 1981). The large size of ganglion cells in aquatic mammals is neither a function of the large size of the eyes nor a function of low cell density. For example, in the elephant, ganglion cell density is less than 400 cells per millimeter square, and cell size does not exceed 35  $\mu\text{m}$  (Stone and Halasz, 1989). The reason why aquatic mammals have large ganglion cells remains unknown and begs further investigation.

**Ganglion Cell Number and Distribution**

The total number of ganglion cells in the manatee’s retina (mean 70,200 in adults) is rather low and less than in any other aquatic mammal reported to date. The

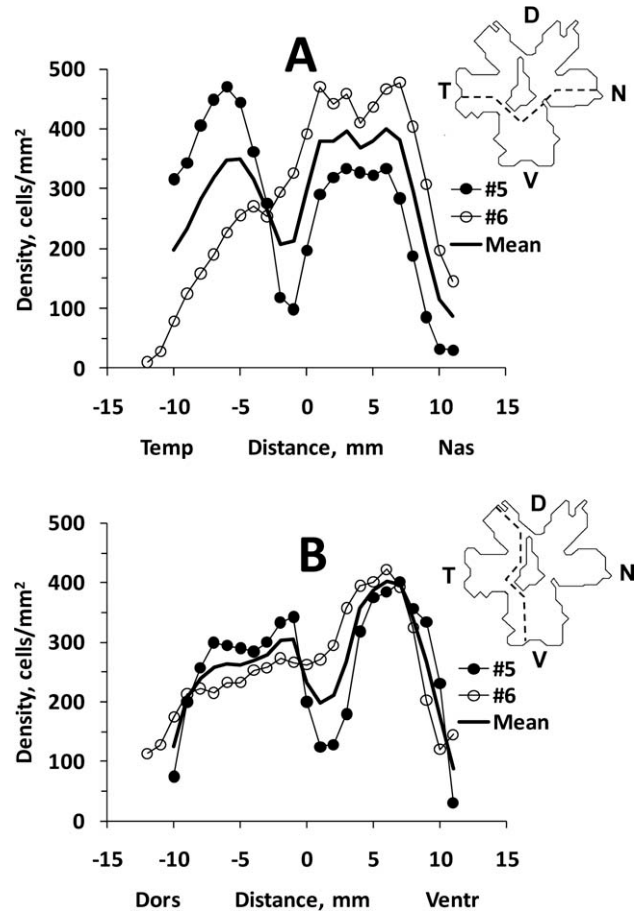


Fig. 10. Ganglion cell density distributions along a nasotemporal line below the optic disc (A) and along a dorsoventral line temporal of the optic disc (B). Plots obtained from two wholemounts (juvenile) and their mean are designated by different symbols. Inserted map contours exemplify the measurement transects in one of the wholemounts (#5 according to Table 1).

number of ganglion cells is 122,000–219,000 in several odontocetes (Mass and Supin, 1995, 2002), 174,000 in mysticetes (Mass and Supin, 1997), 218,000–436,000 in seals (Mass and Supin, 2003, 2010), 177,000–265,000 in sea lions (Mass and Supin, 1992, 2005), and 102,000–111,000 in the walrus (Pütter, 1903; Mass, 1992). Only in the Amazonian dolphin *Inia geoffrensis*, which has notably reduced ocular anatomy and presumably severely limited vision, the number of ganglion cells is less than in the manatee: 14,900–15,500 (Morgane and Jacobs, 1972; Mass and Supin, 1989).

The number of ganglion cells in the manatee is close to that in some terrestrial mammals with moderately developed vision and much smaller body size: 70,000–80,000 in the mouse (Drager and Olsen, 1981) and 76,300 in the hamster (Metin et al., 1995). In other reports on terrestrial mammals, the values are significantly higher: 170,000 in the cat (Wong and Hughes, 1987), 406,000 in the rabbit (Oyster et al., 1981), and 1.5 million in the monkey (Reese and Ho, 1988). These comparisons suggest the manatee’s visual resolution to be inferior to terrestrial mammals.

The data presented here did not reveal definitive areas of high ganglion cell density in the manatee's retina. Nevertheless, some nonuniformity of the cell distribution does exist. Slightly higher cell densities were found in the ventral areas of the wholemounts. This finding is consistent with the observation of Cohen et al. (1982) that ganglion cells are more numerous in the ventral part of the retina. However, the area of increased cell density in the manatee does not look like a clearly delineated area of high cell density as the area centralis or the visual streak in terrestrial mammals.

Qualitatively similar cell distribution patterns as well as overall cell numbers were found in both adult and juvenile retinas. This suggests that in juvenile eyes almost all ganglion cells were differentiated early. As noted above, equivalent cell numbers and cellular packing over a smaller area in the juvenile retina necessarily result in higher cell densities.

The pattern of ganglion cell distribution observed in the manatee's retina is different from that found in most aquatic mammals. Many cetaceans, such as the common dolphin *Delphinus delphis* (Dral, 1983), bottlenose dolphin *Tursiops truncatus* (Dral, 1977; Mass and Supin, 1995), harbor porpoise *Phocoena phocoena* (Mass and Supin, 1986), Chinese river dolphin *Lipotes vexillifer* (Gao and Zhou, 1987), gray whale *Eschrichtius gibbosus* (Mass and Supin, 1997), Dall's porpoise, and Minke whale *Balaenoptera acutorostrata* (Murayama et al., 1992, 1995), have two spots of high cell density, one in the nasal and the other in the temporal retinal quadrants. In pinnipeds, a high cell density area occurs as either a discrete spot (the northern fur seal, Mass and Supin, 1992; the Weddel seal, Welsch et al., 2001) or a streak (the walrus, Mass, 1992) or a combination of both (the sea otter *Enhydra lutris*, Mass and Supin, 2000; the harbor seal, Hanke et al., 2009; the Caspian Seal, Mass and Supin, 2010). All these patterns are different from that found in the manatee. It is notable that in the Amazonian river dolphin the higher cell density area is located in the ventral part of the retina (Mass and Supin, 1989), that is, somewhat similar to that in the manatee. This retinal pattern may be a common feature of aquatic mammals inhabiting low transparency waters, where higher luminance is in the upper part of the visual field (corresponding to the ventral part of the retina).

However, it must also be noted that in all aquatic mammals studied previously, including aquatic mammals with low ganglion cell density, such as *Neophocaena*, *Lipotes* (Gao and Zhou, 1987), and *Inia geoffrensis* (Mass and Supin, 1989), a high cell density area was more evident than in the manatee. Among terrestrial mammals studied to date, only the echidna *Tachyglossus aculeatus* was shown to have a nondifferentiated retina without any specific area of high ganglion cell density (Stone, 1983).

### Ganglion Cell Density and Retinal Resolution

There are two main factors that determine visual acuity: the quality of the optical system of the eye and the retinal resolution. One may expect that these two values are in correspondence; therefore, the retinal resolution may be used as an approximation of visual acuity. A number of investigations have confirmed that retinal resolution estimates based on ganglion cell

density agree well with visual acuity measures in behavioral studies (rev. Pettigrew et al., 1988). In particular, in the domestic cat, which has been the subject of repeated, detailed studies of basic visual mechanisms, close agreement was found between the retinal resolution estimates from ganglion cell density (Hughes, 1985) and behavioral (Jacobson et al., 1976; Mitchell et al., 1977) and evoked-potential (Harris, 1978) results for visual acuity. Among marine mammals, good correspondence has also been found in the bottlenose dolphin between the retinal resolution estimated from ganglion cell densities (Mass and Supin, 1995) and behavioral measures of visual acuity (Herman et al., 1975). Therefore, the data reported here are believed to be satisfactory estimates of the retinal resolution of the manatee.

The ganglion cell density in the ventral part of the manatee's retina was on average as high as 286 cells per millimeter square in adult eyes and 485 cells per millimeter square in juvenile eyes. Assuming that the mean intercellular distance is

$$L = 1/\sqrt{D},$$

where  $L$  is the intercellular distance and  $D$  is the cell density, this corresponds to the mean intercellular distance of 59 and 45  $\mu\text{m}$ , respectively. To convert the intercellular distance to angular measure of visual resolution, the posterior nodal distance of the eye must be known. Underwater, the cornea plays a minor role in ocular refraction. Therefore, the posterior nodal distance of the manatee eye may be considered to be the distance from the lens center to the central part of the retina. This distance was 10.5 mm in adult eyes and 8 mm in juvenile eyes. Retinal resolution is calculated as:

$$V = \frac{L \times 180}{\pi N},$$

where  $V$  is the retinal resolution (angle degree),  $L$  is the intercellular distance, and  $N$  is the posterior nodal distance. Based on this formula, the manatee has a retinal resolution of 0.32-degree angle ( $19'$ ), using both adult and juvenile eye data. This estimate is comparable to the underwater visual acuity found in the behavioral investigation in Florida manatees *Trichechus manatus latirostris* (Bauer et al., 2003), which reported for one subject, in freshwater at 1-m distance, a minimum angle of resolution of  $24'$ , and in saltwater, a best resolution of  $21'$  (nb: a second subject was found to have a much poorer resolution of  $56'$ ).

The data indicate that the retinal resolution and visual acuity of the Florida manatee are markedly lower than that reported in whales and dolphins ( $9'$ – $14'$  by Mass and Supin, 1995, 1997, 1999, 2002) and in pinnipeds ( $3'$ – $8'$  by Mass and Supin, 1992, 2003, 2010; Hanke et al., 2009). It is, however, slightly higher than that in the Amazon river dolphin ( $40'$ – $45'$  by Mass and Supin, 1989). Such a low resolution of the visual system suggests that the manatee is able to distinguish only large objects of great angular size.



Thus, features of the manatee's eye, both those reported previously (vascular corneas and the lack of lenticular accommodation mechanism) and newly reported here (low retinal resolution and low total number of ganglion cells), are consistent with the conclusion that the manatee's vision is only moderately developed.

### ACKNOWLEDGEMENTS

Eyes were collected and transported under U.S. Fish and Wildlife Service Endangered Species Permit PRT-68453 and under CITES Permit US-770760. N.B. Barros (deceased) of the Hubb-Sea World Research Institute and the animal care staff and veterinarians at Sea World of Florida assisted with specimen collection.

### LITERATURE CITED

- Ahnelt PK, Kolb H. 2000. The mammalian photoreceptor mosaic-adaptive design. *Prog Retin Eye Res* 9:711-777.
- Bauer GB, Colbert DE, Gaspard JC, III, Littlefield B, Fellner W. 2003. Underwater visual acuity of Florida manatee (*Trichechus manatus latirostris*). *Int J Comp Psychol* 16:130-142.
- Bertram GCL, Bertram CKR. 1962. Manatees of Guiana. *Nature* 196:1329-1331.
- Cohen JL, Tucker GS, Odell DK. 1982. The photoreceptors of the West Indian manatee. *J Morphol* 173:197-202.
- Collin SP, Pettigrew JD. 1988. Retinal ganglion cell topography in teleosts: a comparison between Nissl-stained material and retrograde labeling from the optic nerve. *J Comp Neurol* 276:412-422.
- Dawson WW. 1980. The cetacean eye. In: Herman LM, editor. *Cetacean behavior: mechanisms and functions*. New York: Wiley. p 53-100.
- Dawson WW, Hawthorne MN, Jenkins RL, Goldston RT. 1982. Giant neural system in the inner retina and optic nerve of small whales. *J Comp Neurol* 205:1-7.
- Drager UC, Olsen JF. 1981. Ganglion cell distribution in the retina of the mouse. *Invest Ophthalmol* 20:285-293.
- Dral ADG. 1977. On the retinal anatomy of cetacea (mainly *Tursiops truncatus*). In: Harrison RJ, editor. *Functional anatomy of marine mammals*. Vol. 3. London: Academic Press. p 81-134.
- Dral ADG. 1983. The retinal ganglion cells of *Delphinus delphis* and their distribution. *Aquat Mamm* 10:57-68.
- Fukuda Y. 1977. A three group classification of rat retinal ganglion cell: histological and physiological studies. *Brain Res* 119:327-344.
- Gao A, Zhou K. 1987. On the retinal ganglion cells of *Neophocaena* and *Lipotes*. *Acta Zool Sin* 33:316-332.
- Gao G, Zhou K. 1992. Fiber analysis of the optic and cochlear nerves of small cetaceans. In: Thomas JA, Kastelein RA, Supin AYA, editors. *Marine mammal sensory systems*. New York: Plenum. p 39-52.
- Griebel U, Peichl L. 2003. Color vision in aquatic mammals-facts and open questions. *Aquat Mamm* 29:18-30.
- Griebel U, Schmidt A. 1996. Color vision in the manatee (*Trichechus manatus*). *Vision Res* 36:2747-2757.
- Griebel U, Schmidt A. 1997. Brightness discrimination ability in the West Indian manatee (*Trichechus manatus*). *J Exp Biol* 200:1587-1592.
- Hanke FD, Peichl L, Dehnhardt G. 2009. Retinal ganglion cell topography in juvenile harbor seals (*Phoca vitulina*). *Brain Behav Evol* 74:102-109.
- Harper JY, Samuelson DA, Reep RL. 2005. Corneal vascularization in the Florida manatee (*Trichechus manatus latirostris*) and three-dimensional reconstruction of vessels. *Vet Ophthalmol* 8:89-99.
- Harris LR. 1978. Contrast sensitivity and acuity of a conscious cat measured by the occipital evoked potentials. *Vision Res* 18:175-178.
- Hartman DS. 1979. Ecology and behavior of the Manatee (*Trichechus manatus*) in Florida. *Am Soc Mamm Spec Publ* 5:153.
- Herman LM, Peacock MF, Yunker MP, Madsen CJ. 1975. Bottlenecked dolphin: double-slit pupil yields equivalent aerial and underwater diurnal acuity. *Science* 189:650-652.
- Hughes A. 1975. A quantitative analysis of the cat retinal ganglion cell topography. *J Comp Neurol* 163:107-128.
- Hughes A. 1981. Population magnitudes and distribution of the major modal classes of cat retinal ganglion cell as estimated from HRP filling and systematic survey of the soma diameter spectra for classical neurons. *J Comp Neurol* 197:303-339.
- Hughes A. 1985. New perspectives in retinal organization. In: Osborne N, Chader G, editors. *Progress in retinal research*. Vol. 4. Oxford: Pergamon Press. p 243-313.
- Jacobson SGK, Franklin BJ, McDonald WI. 1976. Visual acuity of the cat. *Vision Res* 16:1141-1143.
- Landau D, Dawson WW. 1970. The histology of retinas from the pinnipedia. *Vision Res* 10:691-702.
- Mass AM. 1992. Retinal topography in the walrus (*Odobenus rosmarus divergens*) and fur seal (*Callorhinus ursinus*). In: Thomas JA, Kastelein RA, Supin AYA, editors. *Marine mammal sensory systems*. New York: Plenum. p 119-135.
- Mass AM, Odell DK, Ketten DK, Supin AYA. 1997. Ganglion layer topography and retinal resolution of the Caribbean manatee *Trichechus manatus latirostris*. *Doklady Biol Sci* 355:392-394.
- Mass AM, Supin AYA. 1986. Topographic distribution of sizes and density of ganglion cells in the retina of a porpoise, *Phocoena phocoena*. *Aquat Mamm* 123:95-102.
- Mass AM, Supin AYA. 1989. Distribution of ganglion cells in the retina of an Amazon river dolphin *Inia geoffrensis*. *Aquat Mamm* 15:49-56.
- Mass AM, Supin AYA. 1992. Peak density, size and regional distribution of ganglion cells in the retina of the fur seal *Callorhinus ursinus*. *Brain Behav Evol* 39:69-76.
- Mass AM, Supin AYA. 1995. Ganglion cells topography of the retina in the bottlenecked dolphin, *Tursiops truncatus*. *Brain Behav Evol* 45:257-265.
- Mass AM, Supin AYA. 1997. Ocular anatomy, retinal ganglion cell distribution, and visual resolution in the gray whale, *Eschrichtius gibbosus*. *Aquat Mamm* 23:17-28.
- Mass AM, Supin AYA. 1999. Retinal topography and visual acuity in the riverine tucuxi (*Sotalia fluviatilis*). *Mar Mamm Sci* 15:351-365.
- Mass AM, Supin AYA. 2000. Ganglion cell density and retinal resolution in the sea otter, *Enhydra lutris*. *Brain Behav Evol* 55:111-119.
- Mass AM, Supin AYA. 2002. Visual field organization and retinal resolution of the beluga, *Delphinapterus leucas* (Pallas). *Aquat Mamm* 28:241-250.
- Mass AM, Supin AYA. 2003. Retinal topography of the harp seal *Pagophilus groenlandicus*. *Brain Behav Evol* 62:212-222.
- Mass AM, Supin AYA. 2005. Ganglion cell topography and retinal resolution of the Steller sea lion (*Eumetopias jubatus*). *Aquat Mamm* 31:393-402.
- Mass AM, Supin AYA. 2010. Retinal ganglion cell Layer of the Caspian seal *Pusa caspica*: topography and localization of the high resolution area. *Brain Behav Evol* 76:144-153.
- Metin C, Irons WA, Frost DO. 1995. Retinal ganglion cells in normal hamsters and hamsters with novel retinal projection. I. Number, distribution, and size. *J Comp Neurol* 353:179-199.
- Mitchell DE, Giffin F, Timney BN. 1977. A behavioral technique for the rapid assessment of the visual capabilities of kittens. *Perception* 6:181-193.
- Morgane PJ, Jacobs MS. 1972. The comparative anatomy of the cetacean nervous system. In: Harrison RJ, editor. *Functional anatomy of marine mammals*. Vol. 1. New York: Academic Press. p 109-239.
- Murayama T, Fujise Y, Aoki I, Ishii T. 1992. Histological characteristics and distribution of ganglion cells in the retina of the Dall's porpoise and minke whale. In: Thomas JA, Kastelein RA, Supin AYA, editors. *Marine mammal sensory systems*. New York: Plenum. p 137-145.
- Murayama T, Somya H, Aoki I, Ishii T. 1995. Retinal ganglion cell size and distribution predict visual capabilities of Dall's porpoise. *Mar Mamm Sci* 11:136-149.

- Natiello M, Lewis P, Samuelson D. 2005. Comparative anatomy of the ciliary body of the West Indian manatee (*Trichechus manatus*) and selected species. *Vet Ophthalmol* 8:375–385.
- Newman LA, Robinson PR. 2006. The visual pigments of the West Indian manatee (*Trichechus manatus*). *Vision Res* 46:3326–3330.
- Nowak RM, editor. 1991. Walker's mammals of the world. 5th ed. Baltimore: The John Hopkins Press. Vol. 2: p 1298.
- Oyster CW, Takahashi ES, Hurst DC. 1981. Density, soma size and regional distribution of rabbit retinal ganglion cells. *J Neurosci* 1:1331–1346.
- Pettigrew JD, Dreher B, Hopkins CS, McCall MJ, Brown M. 1988. Peak density and distribution of ganglion cells in the retina of microchiropteran bats: implication for visual acuity. *Brain Behav Evol* 32:39–56.
- Piggins D, Muntz WRA, Best RC. 1983. Physical and morphological aspects of the eye of the manatee *Trichechus inunguis* Natterer 1883 (Sirenia: mammalia). *Mar Behav Physiol* 9:111–130.
- Pütter A. 1903. Die Augen der Wassersaugetiere. *Zoologische Jahrbuecher Abteilung fuer Anatomie und Ontogenie der Tiere* 17:99–402.
- Reese BE, Ho KY. 1988. Axon diameter distribution across the monkey's optic nerve. *Neurosciences* 27:205–214.
- Rochon-Duvigneaud A. 1943. Les yeux et la vision des vertebres. Paris: Masson.
- Samuelson DA, Reep RL, Lewis P, Chisholm M. 1994. The ocular anatomy of the West Indian manatee. In: First International Manatee and Dugong Conference. Vol. 1: p 33–34.
- Stone J. 1981. The wholemount handbook. A guide to the preparation and analysis of retinal wholemounts. Sydney: Maitland.
- Stone J. 1983. Topographical organization of the retina in a Monotreme: Australian Spiny Anteater *Tachyglossus aculeatus*. *Brain Behav Evol* 22:175–184.
- Stone J, Halasz P. 1989. Topography of the retina in the elephant *Loxodonta africana*. *Brain Behav Evol* 34:84–95.
- Supin AY, Popov VV, Mass AM. 2001. The sensory physiology of aquatic mammals. Boston: Kluwer.
- Waller G. 1982. Retinal ultrastructure of the Amazon river dolphin (*Inia geoffrensis*). *Aquat Mamm* 9:17–28.
- Walls GL. 1942. The vertebrate eye and its adaptive radiation. Michigan: Cranbrook Institute of Science Bulletin No. 19, Cranbrook Press.
- Welsch U, Ramdohr S, et al. 2001. Microscopic anatomy of the eye of the deep-diving Antarctic Weddell seal (*Leptonychotes weddellii*). *J Morphol* 248:165–174.
- West JA, Sivak JG, Murphy CJ, Kovacs KM. 1991. A comparative study of the anatomy of the iris and ciliary body in aquatic mammals. *Can J Zool* 69:2594–2607.
- Wong ROL, Hughes A. 1987. The morphology, number and distribution of a large population of confirmed displaced amacrine cells in the adult cat retina. *J Comp Neurol* 255:159–177.
- Wong ROL, Wye-Dvorak J, Henry GH. 1986. Morphology and distribution of neurons in the retina ganglion cell layer of the adult Tammar wallaby *Macropus eugenii*. *J Comp Neurol* 253:1–12.